

STRUCTURAL ANALYSIS OF POST-DISASTER MASONRY STRUCTURES MODELED USING CLOUD2FEM SOFTWARE

S. S. Kaushal¹, M. Gutierrez Soto², R. Napolitano¹

¹ Department of Architectural Engineering, Pennsylvania State University, U.S.A – (saanchi.kaushal, nap)@psu.edu

² School of Engineering Design and Innovation, Pennsylvania State University, U.S.A - mvg5899@psu.edu

KEY WORDS: Damage Assessment, Tornado, Historic Masonry, Digital Documentation, Finite Element Analysis

ABSTRACT:

Research often neglects historic and ageing infrastructure when investigating the impact of extreme wind loading and structural strengthening. This is exemplified by the ASCE 7-22 standard in the US that prescribes design loads for tornado hazard, which currently does not apply to Risk Categories (RC) 1 and 2, comprising a significant proportion of historic structures. After a disaster, analyzing these structures numerically can be difficult due to their complex geometries, use of multiple construction materials, and alterations to the original structure. This study aimed to digitally document and evaluate the damage caused by the Midwest Tornado in Kentucky in December 2021, specifically focusing on the historic downtown of Mayfield, KY. Building data was gathered using various devices, such as Unmanned Aerial Vehicle's, LiDARs, and cameras, and converted into finite element meshes using the open-source software Cloud2FEM. Multiple meshes for the historic post office building in Mayfield, KY, was generated using varied rules within Cloud2FEM. These meshes were then simulated using Abaqus to qualitatively assess the stress concentrations observed under tornadic loading calculated using the ASCE7-22.

1. INTRODUCTION

On the 10th of December, 2021, the higher-than-average temperatures (Pappas, 2021), resulted in a tornado outbreak in the southeast region of the United States. This outbreak resulted in the formation of almost 30 tornadoes (Coalition, 2021), out of which the most devastating was the Midwest tornado. The Midwest tornado covered almost 250 miles (Pappas, 2021), leaving a trail of extensive damage in Arkansas, Missouri, Tennessee, and Kentucky. Kentucky (KY) was the worst hit (Schreiner and Lovan, 2021), with some of the impacted towns including Mayfield, Cambridge Shores, Princeton, and Dawson Springs. Tornadoes that occur at night are typically more hazardous and result in a greater number of fatalities, and in Kentucky, nearly 78 casualties were reported. (Pilkington et al., 2021)

To better understand the direct implications of extreme wind loads on historic buildings, this work aims to perform numerical analyses to evaluate the structural performance of the post office from Mayfield, KY, during the Midwest Tornado in December 2021. This historic building was digitally documented during the reconnaissance survey, where the data collected on-site was used to generate point clouds. Multiple approaches are currently developed to explore the transition from a point cloud to a solid mesh for structural analysis. This work examines the application of one such process, i.e., Cloud2FEM. Finite Element Modelling (FEM) is a widely used numerical analysis technique for studying the behavior of masonry structures under various loadings and has been explored here.

High-resolution 3D data capture has become a crucial surveying tool in the last few years and leverages both range-based or image-based techniques (Alfio et al., 2022). The range-based methods, like the Terrestrial Laser Scanner (TLS) uses time-of-flight measurement to ascertain the location of the millions of points, thereby reproducing the structure's geometry (Artese, 2019). Image-based techniques such a photogrammetry extract the points and their locations based on feature extraction and transformation from multiple photographs (Muzzupappa et al.,

2013). In the last few years, these tools have been explored to assess post-disaster damage (Schweier and Markus, 2006), detect changes in the urban layout (Steinle and Bahr, 2003) and monitor structural deformation (Jafari et al., 2017).

The use of point clouds to create numerical models of structures is an increasingly popular research area, with accurate spatial models being essential for structural analysis (Bassier et al., 2019). However, before numerical assessment of buildings can take place, usually a geometric replica of the structure is constructed using Computer-Aided Design (CAD), which can be time-consuming and often results in a simplified model (Castellazzi et al., 2017). For example, a researcher developed hybrid point cloud, using both TLS and photogrammetry, drew a CAD model and then ran their numerical analysis (Aguilar et al., 2019). Similarly, Napolitano et al., used laser scanners to capture the geometry of cracks present in the foundation, and apply the CAD approach to simulate the finite-distinct element model and reproduce the damage indicator (i.e., cracks) (Napolitano et al., 2019).

To reduce the time and effort required to produce CAD models, research has been conducted to identify ways to bypass the CAD method for structural analysis. Barsanti and Guidi (Barsanti and Guidi, 2018) proposed a surface modelling approach that converts the point into a volumetric mesh, providing higher accuracy during simulations. Meanwhile, Hinks et al. (Hinks et al., 2013) use a voxelization method to transform the point cloud into solid models, specifically for facades. Castellazzi et al. (Castellazzi et al., 2022) also used the voxelization method to generate finite element models from point clouds, developing a semi-automatic software to do so.

1.1 Case Study: Mayfield

The focus of this project is the US Post Office in Mayfield, which was selected as the case study due to the extensive damage it sustained during the Midwest tornado outbreak in December 2021. The severity of a tornado is typically measured by the

level of destruction inflicted on the affected areas, according to the Enhanced Fujita (EF) Scale (McDonald et al., 2010). In this case, the tornado was classified as an EF-4, which indicates significant damage to buildings, with EF-0 being the least severe and EF-5 being the most destructive category. Figure 1 illustrates the various damages in the post office after the Midwest tornadoes.



Figure 1. The post office in Mayfield before (top: August 2019) and after (bottom: December 2021) the disaster

To collect the necessary data, a two-phase approach was employed. The first phase involved conducting a large-scale damage assessment as part of the Structural Extreme Events Reconnaissance Network (Pilkington et al., 2021). This allowed for identifying the most severely impacted areas, including Mayfield. The second phase involved on-site data collection of the historic buildings in Mayfield, using high-resolution 3D data capture techniques. This was undertaken in March 2022, almost 3 months after the disaster struck.

Mayfield, Kentucky, was established in 1821 to serve as a center for government, social, and commercial activities (Places, 1984). The construction of the public square in 1824 and the installation of railroads during the mid-1800s contributed to the town's expansion between 1875 and 1934, along with increased textile and tobacco business (Munday, 1925). The town's historic downtown showcases various architectural styles seen in Victorian and Classical masonry construction, which was a common technique used in the country between 1800 and 1940 (Rabun, 2000). Due to its early town planning and architectural significance, the historic district was added to the National Register of Historic Places in 1984, with the registration being updated in 1996 to include relevant surrounding buildings that also contributed to the town's character and history (Places, 1996).

2. RESEARCH AIM

The present work aims to evaluate the structural performance of the historic masonry US Post Office in Mayfield, Kentucky

impacted by the Midwest Tornadoes in December 2021. This structure was digitally documented using high-resolution 3D data capture techniques, and a representative finite element model was generated using Cloud2FEM. While using Cloud2FEM, meshing parameters were varied to qualitatively understand the change in the numerical response of the mesh.

3. METHODOLOGY

The methodology for this project adopted a three-phased approach. The data collection was the focus of the first phase, followed by the processing of the data in the second phase, and the generation of the finite element model in the third phase. Each of these phases is further elaborated in the following sections.

3.1 Data Acquisition

The data acquisition approach was decided based on a priority list generated for the relevant structures. As a part of this paper, the specific details for the Mayfield Post Office have been listed below. The data for the post office was collected over a period of a few days, in March 2021, using both range-based and image-based techniques. The Leica RTC360 was used as the range-based, and can accurately capture data at a rate of 2 million points per second, creating a point cloud in less than two minutes (Biasion et al., 2019). The TLS was set up at every corner of the post office, and in the middle when the external walls were more detailed. In totality, there were 8 scans collected for the post office.

As a part of the image-based data collection, an Unmanned Aerial Vehicle (UAV), was used for taking aerial imagery. Specifically for the post office, the DJI Matrice was flown in a grid-like pattern to collect these images. A hand-held camera, Cannon DSLR helped capture on-ground images and augment the aerial images. There were over 400 images captured aerially and 1600 from the ground.

Even though TLS has been deemed to be more precise (Meng et al., 2010), these techniques complement each other and provide more accurate results when integrated (Baltsavias, 1999). Thus, this data collected from the post office was concatenated to achieve an exact replica of the structure and the process has been explained in the next section.

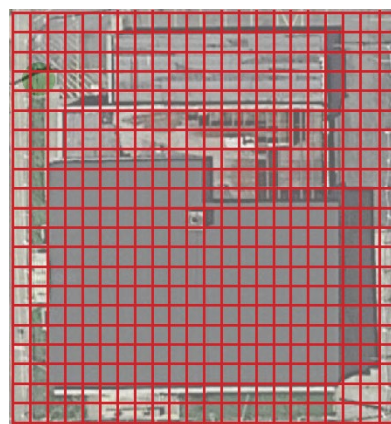


Figure 2. The UAV flight path for the post office

3.2 Data Processing

The data processing involved a three-step approach, where the first two focused on creating separate point clouds for the UAV



Figure 3. The substeps for fusing the data together

and LiDAR data. The third step of the process aimed at combining these two point clouds and an overview of this is provided in Figure 3. The UAV images were processed using Pix4D, a photogrammetry software used for constructing point clouds (PIX4D, 2022). Once the images are uploaded to the software, the three processing steps are executed to generate the point cloud. During the ‘initial processing’, the images are calibrated and oriented spatially based on the ground control points (GCP). For the post office, there were 4 GCP points used to position the images in a 3D space. The following two steps, the ‘point cloud and mesh’ and the ‘DSM, Orthomosaic and Index’, run successfully without human intervention and generate the final model. Figure 4 shows the point cloud generated by Pix4D, where some portions of the post office were missing, specifically on the roof and wall bases. This was due to reflection from stagnant water or the UAV not capturing enough images.

The LiDAR scans were imported into Leica’s Register360; this was a straightforward process since the RTC360 was also a Leica product. Once the 8 scans were imported, they were aligned in pairs to ensure that their overlap was more than 99.5%. Figure 5 displays the aligned scans for the post office. As mentioned previously, the UAV point cloud had missing sections that were supplemented by the LiDAR point cloud and has been explained in the following section.

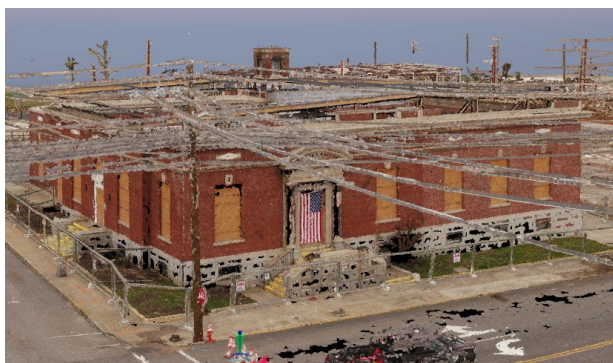


Figure 4. The final point cloud for the Post Office from Pix4D

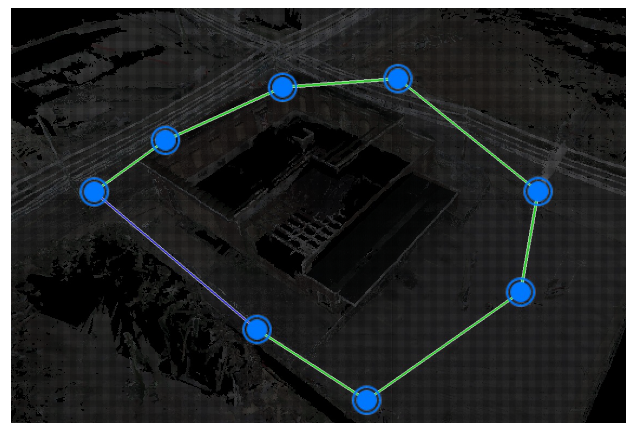


Figure 5. The aligned scans for the Post Office from Register360

3.3 Fusing the Point Clouds

Combining point clouds for digital documentation is often considered more reliable and precise than using a single point cloud. One method of merging LiDAR and UAV data is through registration techniques, which align corresponding points from both point clouds and combine them into a complete 3D model. The iterative closest point (ICP) algorithm is a commonly used registration technique introduced by Besl and McKay (BeslPJ, 1992), which matches corresponding points and calculates a transformation matrix to minimize the distance between points repeatedly. Once the point clouds were processed separately, Cyclone software merged them (Leica Geosystems, 2022). Cyclone, developed by Leica, is a software package that processes point cloud data, including registration and fusion. The primary advantage of using this software was its rapid integration with the point clouds consolidated in Cyclone Register 360, which was used to process the LiDAR data.

In the Cyclone software, the merging of the two point clouds occurs following registration and alignment. The registration process involves matching the point clouds based on a common co-ordinate system, which can be achieved through manual, automatic, or hybrid approaches. In manual registration, the user identifies corresponding points between the point clouds and

separates them later for alignment. On the other hand, the automated approach uses an algorithm to identify these points automatically. The hybrid approach combines both methods, allowing the software to automatically classify corresponding points automatically while the user can manually add more points. After the point clouds are registered, they are aligned. The alignment options available in cyclone include plane-to-plane, feature-to-feature, and best-fit alignment. The plane-to-plane method aligns the two point clouds based on their dominant planes, the feature-to-feature aligns the point clouds based on corresponding features such as edges and the best-fit alignment tries to minimize the distance between the two point clouds. Once the point clouds are aligned, they are merged into one point cloud.



Figure 6. The unaligned point clouds

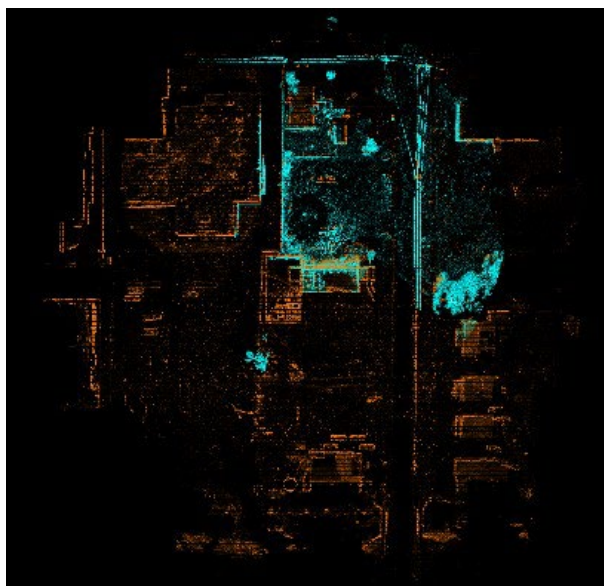


Figure 7. The aligned point clouds

Working with the Mayfield Post Office, a hybrid approach was used to register the two point clouds. The point cloud generated in Pix4D was imported as a complete point cloud, while the LiDAR scans were imported as separate scans, even though they had been previously aligned in Register 360. All the LiDAR scans were individually registered with the point cloud and aligned using Cyclone's auto-alignment, which produced an error of up to 20cm. Following this, each of these scans-to-pointcloud were manually aligned to reduce the alignment error. This was a time-consuming step, where aligning one scan would affect the error for all the scans. The final error was minimal and is mentioned in Table 1, where the higher errors were

observed in the damaged walls. It should be emphasized that since this data was collected from a disaster site with a lot of debris, these minimal errors may be ignored for now.

Wall 1	Wall 2	Wall 3	Wall 4	Roof
0.025m	0.05m	0.017m	0.06m	0.007m

Table 1. The final errors for each wall of the Post Office

3.4 Generate a Finite Element Model

Finite element analysis (FEA) is one of the most common methods to simulate the structure under varied loading and understanding their response. Two primary methods for generating finite element meshes from point clouds are either using meshing software that utilizes algorithms to create a mesh that conforms to the point clouds (Suchde et al., 2023), or utilizing the point cloud to draw the structures and transform it into a finite mesh (Takhirov et al., 2017, Aguilar et al., 2019).

The finite element mesh for this project was generated using Cloud2FEM, a semi-automatic software developed by Castellazzi et al. (Castellazzi et al., 2022) that was previously mentioned. This software effectively utilized the point clouds to create dense finite element models. The point cloud was initially sliced vertically into a user-defined number of slices, with a closed polygon extracted for each of these slices by connecting the internal and external wall points within the software. The resulting slices were then stacked vertically to produce a 3D voxelized object. Each voxel was converted into an 8-node hexahedral element to obtain a 3D solid mesh. Further information on this process and the software is available in the following references (Castellazzi et al., 2022, Lambertini, 2015, Castellazzi et al., 2017).

Given its direct usage of point clouds and its integration with ABAQUS, Cloud2FEM was employed to transform the Mayfield Post Office point cloud into a finite element mesh. The point cloud was imported in .ply format, and after importation, the software's graphical interface displayed the Zmax and Zmin coordinates of the point cloud, which represent the height of the point cloud. Subsequently, the user has the option to choose between two slicing rules, namely the fixed number of slices or the fixed step height. For this project, the 'fixed number of slices' rule's configuration has been varied to understand the impact of it on the overall simulation, and the following combinations were attempted:

- A: slices = 26, slice thickness = 1m
- B: slices = 13, slice thickness = 1m
- C: slices = 26, slice thickness = 0.5m

Centroids were generated for each slice after the point cloud was sliced. This process effectively reduced excessive noise and made the slices more ordered, which aided in constructing cleaner polylines. During the simulation of the Mayfield Post Office, it took up to 2 days to produce the centroids when the slices were not cleaned. Removing random points from each slice before initiating this step is recommended to reduce the computation time required to generate the centroids.

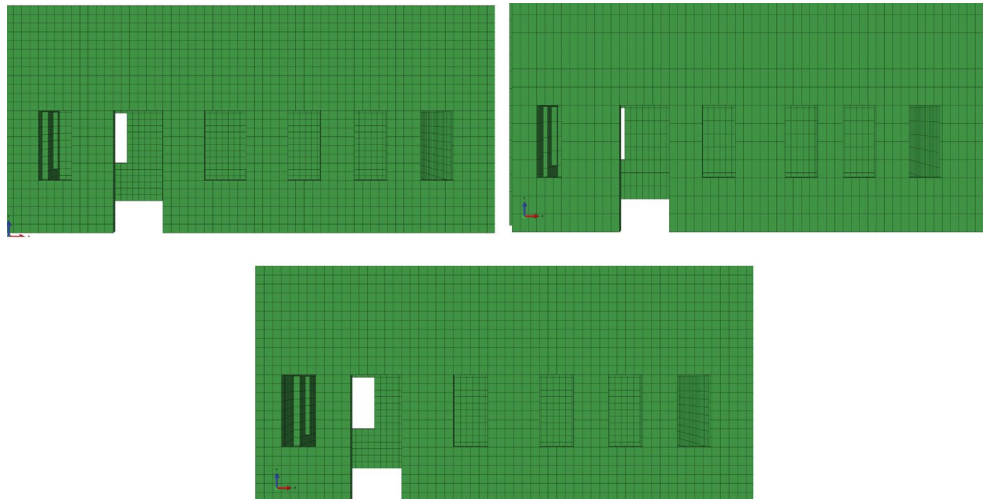


Figure 8. The different meshes generated from cloud2fem, A & B (top), C (bottom)

Once the centroids were generated, polylines for the polygons were created, which required no human intervention. The most time-consuming step of the process began after the raw poly-lines were created, which involved cleaning them and ensuring that they followed the geometry of the sliced point cloud. After the polylines were cleaned, the polygons were formed and meshed. It is worth noting that the mesh size is dependent on the slice thickness and the grid defined in the graphical user interface (GUI).

Figure 8 represents the three different meshes generated for the post office. Visually, there were multiple differences observed in the final meshes. The first, the size of the finite element was dependent on the number of slices and the grid dimensions while cleaning the polylines. The second, was in the roof plans as seen in Figure 9. The difference in slice thicknesses alters the number of points in each slice, this in turn changes poly-lines which alters the geometry of the polygons that are generated. This difference in the roof of A, B and C was possibly a result of cleaning the polylines with different slice thicknesses. Given this, the slice thickness of 1m seems reasonable for the proposed study since the final mesh was a geometric replica of the actual structure.

3.5 Finite Element Model Material Properties

After generating the final meshes (Figure 8), an examination was conducted to analyze how parameters of the point cloud to FEM process affects the structural behavior. In ABAQUS, several constitutive models are available to replicate the mechanical characteristics of masonry, such as Smeared Crack Concrete, Brittle Crack Concrete, or Concrete Damage Plasticity (CDP). For this particular study, the CDP model was utilized since it models different strengths in tension and compression and has been previously applied to masonry with successful results (Acito et al., 2014, Tiberti et al., 2016). The CDP model relies on hyperbolic functions of Drucker-Prager and requires a predefined set of parameters to function properly. These parameters comprise eccentricity parameters (set to 0.1), a dilation angle of 20, the ratio between bidirectional and unidirectional compressive strength of masonry (1.16), and a viscosity parameter of 0.02 (Lubliner et al., 1989). The input properties for the CDP model's compressive and tensile behavior were obtained from Motovali et al. (Motovali Emami et al., 2017), and used for the current simulations.

4. ANALYSING THE FINITE ELEMENT MODEL

The finite element model in the simulations was exposed to tornado loads estimated using the ASCE 7-22 current standard. To carry out this study, the post office was considered a Risk Category III structure as the current code does not include Risk Category II structures for calculating tornado loads. Estimating wind speeds is often based on multiple damage indicators, and can vary extensively in the same region (Rhee et al., 2022).

Despite the code specifying wind speeds corresponding to an EF0-EF2 intensity tornado, the study evaluated stress concentration variations in the different meshed resulting from the applied load. The wind speeds were estimated based on ASCE7-22 at 35.45 m/s for a 1,700 mean return interval (American Society of Civil Engineers, 2022).

The loading conditions were established for the main wind force resisting system and the roof using the wind speeds, and stress values were estimated by applying them to the finite element model. The loads were applied to the rear wall of the post office, calculated using the aforementioned wind speeds in accordance with ASCE7-22, which accounted for winds impacting the structure from any direction. The positive and negative pressures generated by the tornado wind speeds were manually computed across the entire surface area of the wall and roof. These loads were then estimated for each node by dividing the total pressure by the number of nodes present in the wall and roof.

The primary difference between the meshes during the simulations was the computational time and the accuracy of the results. Mesh A, being coarser, was computationally faster compared to mesh B and C. Since the post office was a relatively simple geometric structure without any complexities, both mesh sizes accurately represented the structure.

Mesh	Number of Elements	Simulation Time
A	13983	174s
B	8717	9s
C	14007	170s

Table 2. Computation time for the analysis

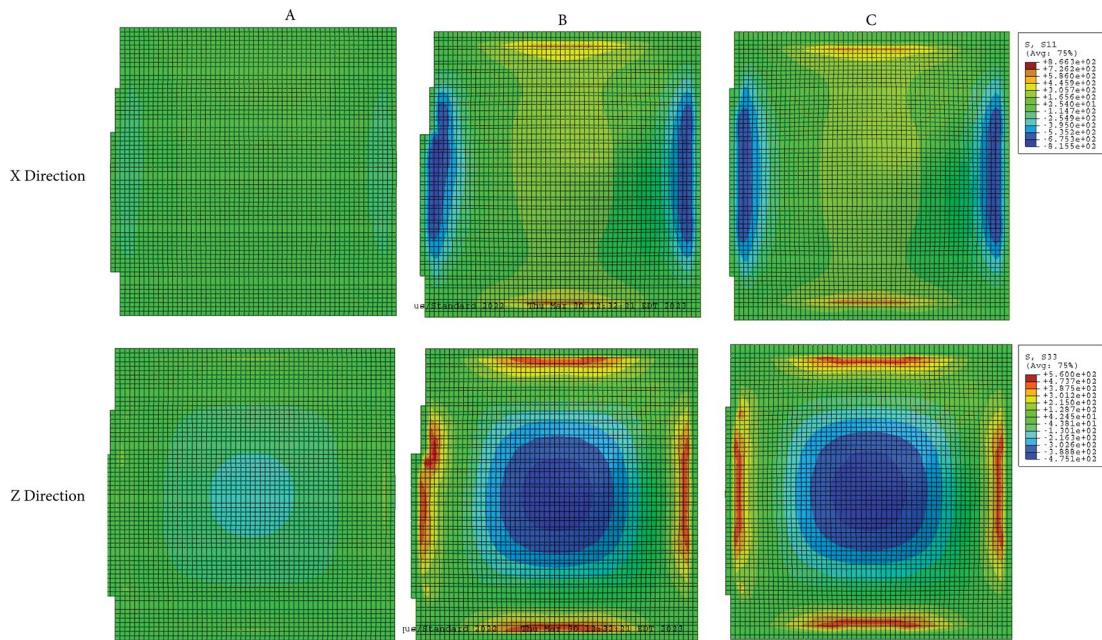


Figure 9. The stress concentrations in x and z direction for the meshes different meshes

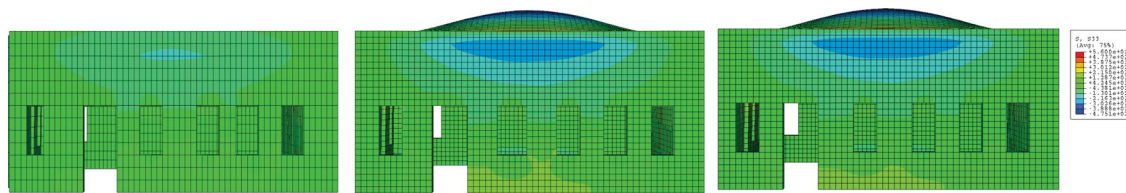


Figure 10. The uplifts observed in the meshes (L-R: A,B,C)

Figure 9 illustrates the initial results for the roof, showing the stresses observed under loading conditions in all directions X and Z. It is noteworthy that regardless of the direction being evaluated, meshes B and C exhibited higher stress values than A when plotted for comparable limits. This suggests that the mesh dimensions for mesh A were possibly too coarse for the simulation and would need to be refined in the future to view any stress concentrations. The stresses in the Z direction depict roof uplift during a tornado, which is one of the most common damages observed in post-disaster reconnaissance (Roueche and Prevatt, 2013).

5. CONCLUSION

Severe weather events like tornadoes can cause significant damage to buildings and structures, leaving them susceptible to failure. The post office building in Mayfield, KY, was one of many structures that suffered extensive damage during the Midwest tornado in December 2021. To assess the behavior of this historic building under extreme wind loads, researchers used point cloud technology to capture high-resolution 3D data, which was then converted into a finite element mesh using Cloud2FEM, an open-source software. This approach saves time by avoiding the need to create a CAD model, which may be less accurate.

The use of point clouds to create numerical models of structures is a rapidly growing research area, with various approaches being developed to explore how to transition from a point cloud to a solid mesh for structural analysis. Even though there are multiple approaches present for this conversion, the final geometry would need to be verified for the documented structure. The coarse and fine mesh generated by Cloud2FEM were in ABAQUS to determine their stress concentrations, using tornado loads calculated based on ASCE7-22 standards. These simulations showcased the need for a selecting an appropriate mesh to qualitatively assess any damage. In the future, the models need to be validated using wind load estimates captured from national weather services, or experimental data for quantitative damage assessment with higher confidence levels.

ACKNOWLEDGEMENTS

This material is based upon work supported by the National Science Foundation under Grant No.IIS-2123343 and CMMI 2222849. Any opinions, findings, and conclusions or recommendations expressed in this material do not necessarily reflect the views of the National Science Foundation. The authors would like to express their gratitude to RAPID Facility at the University of Washington and the research students from

Penn State University, for their support with the data collection and processing during this research project. This material was also supported by the work done by Keely Patelski from Texas Tech University.

REFERENCES

- Acito, M., Bocciarelli, M., Chesi, C., Milani, G., 2014. Col-lapse of the clock tower in Finale Emilia after the May 2012 Emilia Romagna earthquake sequence: Numerical insight. *Engineering Structures*, 72, 70–91.
- Aguilar, R., Noel, M. F., Ramos, L. F., 2019. Integration of reverse engineering and non-linear numerical analysis for the seismic assessment of historical adobe buildings. *Automation in construction*, 98, 1–15.
- Alfio, V. S., Costantino, D., Pepe, M., Restuccia Garofalo, A., 2022. A Geomatics Approach in Scan to FEM Process Applied to Cultural Heritage Structure: The Case Study of the "Colossus of Barletta". *Remote Sensing*, 14(3), 664.
- American Society of Civil Engineers, 2022. *Minimum Design Loads and Associated Criteria for Buildings and Other Structures*. Asce/sei 7-22 edn, American Society of Civil Engineers.
- Artese, S., 2019. THE Survey of the san francesco bridge by santiago calatrava in cosenza, Italy. *The International Archives of Photogrammetry, Remote Sensing and Spatial Information Sciences*, 42, 33–37.
- Baltsavias, E. P., 1999. A comparison between photogrammetry and laser scanning. *ISPRS Journal of photogrammetry and Remote Sensing*, 54(2-3), 83–94.
- Barsanti, S. G., Guidi, G., 2018. A new methodology for the structural analysis of 3d digitized cultural heritage through fea. *IOP Conference Series: Materials Science and Engineering*, 364number 1, IOP Publishing, 012005.
- Bassier, M., Hardy, G., Bejarano-Urrego, L., Drougkas, A., Verstryngge, E., Van Balen, K., Vergauwen, M., 2019. Semi-automated creation of accurate fe meshes of heritage masonry walls from point cloud data. *Structural Analysis of Historical Constructions: An Interdisciplinary Approach*, Springer, 305–314.
- BeslPJ, M., 1992. AMethodforRegistrationof3 DShapes. *IEEETransactionsonPatternAnalysisand MachineIntelligence*, 14(2), 239.
- Biasion, A., Moerwald, T., Walser, B., Walsh, G., 2019. A new approach to the Terrestrial Laser Scanner workflow: the RTC360 solution. *FIG Working Week 2019: Geospatial Information for a Smarter Life and Environmental Resilience*.
- Castellazzi, G., D'Altri, A. M., de Miranda, S., Ubertini, F., 2017. An innovative numerical modeling strategy for the structural analysis of historical monumental buildings. *Engineering Structures*, 132, 229–248.
- Castellazzi, G., Presti, N. L., D'Altri, A. M., de Miranda, S., 2022. Cloud2FEM: A finite element mesh generator based on point clouds of existing/historical structures. *SoftwareX*, 18, 101099.
- Coalition, N. L. I. H., 2021. Extreme tornado outbreak devastates portions of midwest and tennessee valley. National Low Income Housing Coalition.
- Hinks, T., Carr, H., Truong-Hong, L., Laefer, D. F., 2013. Point cloud data conversion into solid models via point-based voxelization. *Journal of Surveying Engineering*, 139(2), 72–83.
- Jafari, B., Khaloo, A., Lattanzi, D., 2017. Deformation tracking in 3D point clouds via statistical sampling of direct cloud-to-cloud distances. *Journal of Nondestructive Evaluation*, 36, 1–10.
- Lambertini, A., 2015. From laser scanning to finite element analysis of complex building by using a semi-automated procedure. *Sensors*, 15, 18360–18380.
- Leica Geosystems, 2022. Leica Cyclone. <https://leica-geosystems.com/en-us/products/laser-scanners/software/leica-cyclone>.
- Lubliner, J., Oliver, J., Oller, S., Onate, E., 1989. A plastic-damage model for concrete. *International Journal of solids and structures*, 25(3), 299–326.
- McDonald, J. R., Mehta, K. C., Smith, D. A., Womble, J. A., 2010. The enhanced fujita scale: Development and implementation. *Forensic Engineering 2009: Pathology of the Built Environment*, 719–728.
- Meng, X., Currit, N., Zhao, K., 2010. Ground filtering algorithms for airborne LiDAR data: A review of critical issues. *Remote Sensing*, 2(3), 833–860.
- Motovali Emami, S. M., Mohammadi, M., Lourenc,o, P. B., 2017. Equivalent diagonal strut method for masonry walls in pinned connection and multi-bay steel frames. *Journal of Seismology and Earthquake Engineering*, 19(4), 299–311.
- Munday, J., 1925. The railroads of Kentucky 1861-1865.
- Muzzupappa, M., Gallo, A., Spadafora, F., Manfredi, F., Bruno, F., Lamarca, A., 2013. 3d reconstruction of an outdoor archaeological site through a multi-view stereo technique. *2013 Digital Heritage International Congress (DigitalHeritage)*, 1, IEEE, 169–176.
- Napolitano, R. K., Hess, M., Glisic, B., 2019. The foundation walls of the Baptistery Di San Giovanni: a combination of laser scanning and finite-distinct element modeling to ascertain damage origins. *International Journal of Architectural Heritage*, 13(7), 1180–1193.
- Pappas, S., 2021. Quad-state tornado may be longest-lasting ever. *Scientific American*.
- Pilkington, S., Roueche, D., Gutierrez Soto, M., Alam, M., Napolitano, Rebecca; Kijewski-Correa, T., Prevatt, D., Kaushal, S. S., Nakayama, J., Saleem, M. R., Ibrahim, H., Lyda, A., Lester, H., Caballero Russi, D., Gurley, K., Robertson, I., Lom-bardo, F., 2021. Steer: 10 december 2021 mid-west tornado out-break joint preliminary virtual reconnaissance report and early access reconnaissance report (pvrr-earr). Technical report.
- PIX4D, 2022. PIX4d Mapper. <https://www.pix4d.com/>.
- Places, N. R. O. H., 1984. National register of historic places nomination form: Mayfield downtown commercial district (boundary increase).

Places, N. R. O. H., 1996. National register of historic places nomination form: Mayfield downtown commercial district (district expansion).

Rabun, J. S., 2000. *Structural Analysis of historic buildings: Restoration, preservation, and adaptive reuse applications for Architects and Engineers*. John Wiley & Sons.

Rhee, D. M., Nevill, J. B., Lombardo, F. T., 2022. Comparison of Near-Surface Wind Speed Estimation Techniques Using Different Damage Indicators from a Damage Survey of Naplate, IL EF-3 Tornado. *Natural Hazards Review*, 23(1), 04021052.

Roueche, D. B., Prevatt, D. O., 2013. Residential damage patterns following the 2011 Tuscaloosa, AL and Joplin, MO tornadoes. *J. Disaster Res*, 8(6), 1061–1067.

Schreiner, B., Lovan, D., 2021. Kentucky tornado toll in dozens; less than feared at factory. <https://apnews.com/article/tornadoes-kentucky-illinois-arkansas-tennessee-missouri-e1ae21e0b7521c28411f8c360b756700>.

Schweier, C., Markus, M., 2006. Classification of collapsed buildings for fast damage and loss assessment. *Bulletin of earthquake engineering*, 4, 177–192.

Steinle, E., Bahr, H., 2003. Detectability of urban changes from airborne laser scanning data. *INTERNATIONAL ARCHIVES OF PHOTOGRAMMETRY REMOTE SENSING AND SPATIAL INFORMATION SCIENCES*, 34(7/B), 1135–1140.

Suchde, P., Jacquemin, T., Davydov, O., 2023. Point cloud generation for meshfree methods: An overview. *Archives of Computational Methods in Engineering*, 30(2), 889–915.

Takhirova, S., Gilani, A., Quigley, B., Myagkova, L., 2017. Detailed numerical analysis of a historic building based on its current condition captured by laser scans and material tests. *6th ECCOMAS thematic conference on computational methods in structural dynamics and earthquake engineering, Rhodes Island, Greece*.

Tiberti, S., Acito, M., Milani, G., 2016. Comprehensive FE numerical insight into Finale Emilia Castle behavior under 2012 Emilia Romagna seismic sequence: Damage causes and seismic vulnerability mitigation hypothesis. *Engineering Structures*, 117, 397–421.